The Thermal Balance of the Lower Atmosphere of Venus

Martin G. Tomasko

Lunar and Planetary Laboratory

University of Arizona

Tucson, Arizona 85721

December 15, 1981

For submission to Venus (Hunten, D. M., Colin, L., and Donahue, T. M., eds.)

Abstract

Since the late 1950s, the temperature near the surface of Venus (now established at 730 K) has been known to be remarkably high in view of Venus's cloud cover which causes the planet to absorb even less sunlight than does Earth. Early attempts to understand the thermal balance that leads to this unusual state were hindered by the lack of basic information regarding the composition, temperature-pressure structure, cloud properties, and wind field of the lower atmosphere. Beginning in the 1960s, a series of successful space missions has measured many of the above quantities that control the transfer of heat in Venus's lower atmosphere. In this chapter, the relevant observational data are summarized and the attempts to understand the thermal balance of Venus's atmosphere below the cloud tops are reviewed. The current data indicate that sufficient sunlight penetrates to deep atmospheric levels and is trapped by the large thermal opacity of the atmosphere to essentially account for the high temperatures observed. Nevertheless, several features, particularly those due to atmospheric dynamics, remain to be understood.

In order to understand the thermal balance of the lower atmosphere of Venus, we must evaluate the rates of various processes that can transport heat in this region. To know these rates, we need to have detailed information regarding the composition, temperature-pressure structure, clouds, and dynamical state of the atmosphere. For the lower atmosphere of Venus, loosely defined here as the region below the cloud tops, this information was especially meager before the advent of space missions to the planet. In the past decade or so, however, a series of remarkably successful Mariner, Venera, and Pioneer missions has advanced our knowledge to the point where separate review chapters in this book are devoted to each of these topics. Accordingly, while our understanding is still incomplete, we have finally measured or are in a position to quantitatively evaluate some of the heat transport rates we believe should be most important in this no longer inaccessible portion of the Venus atmosphere.

The earliest available data bearing on the thermal balance of Venus concerned its size, distance from the Sun, and albedo. The data suggested that while Venus is closer to the Sun than is Earth, it also has a more complete cloud cover than Earth's, with the result that Venus absorbs an amount of sunlight that is somewhat less than that absorbed by the Earth. Judging by conditions on Earth, Venus's extensive cloud cover suggested the presence of a considerable amount of water, and for some years the popular conception of Venus was of a planet with a climate similar to that of the Earth, a view gradually revealed to be far from true.

Section I of this chapter reviews our growing knowledge of the conditions in the lower atmosphere of Venus which bear on its thermal balance. These conditions include the temperature profile, cloud structure and optical properties, composition, and wind field. Section II relates the heating and

cooling rates to several of the observed atmospheric parameters (radiative flux profiles, cloud and atmospheric structure), and briefly reviews some of the major developments in attempts to model the thermal balance of Venus's lower atmosphere. Present problems and areas requiring further work are indicated.

I. Summary of Relevant Observations

A. Temperature Structure

An estimate of the temperature in the cloud-top region of Venus's atmosphere can be obtained from the relative strengths of absorption lines arising from different rotational levels in the near infrared region of Venus's spectrum using observations made from Earth. Results using a homogeneous scattering model give temperatures of 240 to 270 K and a pressure of about 0.2 bar as typical of cloud-top conditions (Belton 1969), values not grossly different from cloud top conditions on Earth.

However, the characteristics of the microwave emission from Venus, first detected by Mayer (1958), greatly changed our view of conditions on Venus (Chapter 4). In the spectral range between 2 and 20 cm, Venus was seen to emit radiation at a roughly constant brightness temperature of about 600 K. In 1962 limb darkening observations at 1.9 cm by Mariner 2 indicated that this emission indeed originated from the surface of the planet and not from some unusual phenomenon in the upper atmosphere. In 1967 the combined radio occultation measurements of Mariner 5, direct entry measurements from Venera 4, and earth-based radar observations of the radius of Venus were sufficient to yield a surface pressure of $\gtrsim$ 70 bars and a surface temperature of about 700 K. Direct measurements by a series of entry probes beginning with Venera 7 have confirmed the remarkably high temperature and pressure near the surface of Venus (Marov 1972; Marov et al. 1973a,1976).

Among the most accurate measurements of the temperature-pressure structure of the lower atmosphere of Venus are those made on the four Pioneer Venus (PV) probes (Seiff et al. 1980; Chapter 11 in this book). The probe entry locations are shown in Fig. 1 and vary in latitude from 30°S to 60°N and in solar zenith angle (SZA) from 66° to 150°. The close agreement between the atmospheric structures observed at these sites is apparent in the figure. The day and night probe temperature profiles are essentially equal between 20 and 35 km altitude, while their differences show a wave with an amplitude of a few degrees K between 35 and 65 km. The mean temperature profiles at these altitudes are very nearly equal at the day and night probe sites. The wave appears also in the temperature difference profiles of the Day-North and Day-Large probe sites, but superimposed on a general trend that has the North probe profile becoming 20 K cooler and the Large probe a few degrees warmer than the Day probe at 65 km altitude (see Seiff et al. 1980; Chapter 11).

The profiles of static stability in the lower atmosphere at the four PV probe sites are shown in Fig. 2. The atmosphere exhibts a subadiabatic (stable) temperature gradient above the clouds, and becomes neutrally stable in the middle cloud. At all four sites, the atmosphere exhibits a markedly stable profile from the cloud bottom at about 50 km down to about 30 km altitude. The adiabatic profile is then followed down to altitudes of about 20 km, below which several of the profiles again indicate a return to stable conditions before the data from the temperature sensors on all four probes terminate at 13 km altitude. These data regarding static stability are especially useful for constraining models of the thermal balance of Venus's lower atmosphere.

B. Absorption of Sunlight

There are at least two separate problems concerning the absorption of sunlight: the variation of absorbed energy with wavelength and the variation with height. The variation with wavelength of the spherical albedo of Venus was obtained by Irvine (1969) from observations at many phase angles at each of a variety of narrow spectral bands from the near ultraviolet to the near infrared. From these data the bolometric spherical albedo was estimated as 0.77 ± 0.07 with the uncertainty largely due to the uncertainty in the magnitude of the Sun. The high value of the albedo A implies a small and relatively uncertain value for the amount of absorbed solar energy, which is proportional to $(1 - A) = 0.23 \pm 0.07$. If Venus is in equilibrium with absorbed sunlight, it should emit 150 ± 45 W m^{-2} corresponding to an effective temperature of 227^{+15}_{-20} °K. The albedo of Venus is very high in the visible, but drops in the ultraviolet and is quite low at wavelengths longward of 1 μm due to absorption by carbon dioxide and the cloud particles. Since a considerable fraction (about 1/3) of the Sun's energy is found at wavelengths longward of 1 μm, this region is responsible for a large fraction (about half) of the solar energy absorbed by Venus. In the visible, where the sun's output is largest, the albedo of Venus is uncertain but high, on the order of 0.90 or greater. Thus, relatively little of the sunlight absorbed by Venus is at wavelengths between 0.6 and 0.9 μm. Shortward of 0.5 μm, the albedo decreases rapidly, and despite the decreasing brightness of the Sun, a substantial fraction (about 35%) of the energy absorbed by Venus is found at wavelengths shortward of 0.5 μm.

Because Venus's albedo is so low in the ultraviolet and near infrared where Venus absorbs most of its solar energy, much (about half) of the sunlight absorbed by Venus is absorbed at moderately high altitudes (above the cloud tops at ~ 65 km) (A. Young 1975). What is less clear is how deep the

remaining sunlight penetrates before being absorbed. This profile is almost impossible to estimate without direct measurements from entry probes.

The first measurements of the penetration of sunlight in the atmosphere of Venus were made from Venera 8 (Avduevsky et al. 1973). These data consisted of measurements of the downward flux of sunlight between about 0.5 and 0.8 μm from 48 km altitude to the surface. While only about 10% of the solar energy absorbed by Venus is contained in this wavelength range, it is at these wavelengths that solar radiation penetrates most deeply into Venus's atmosphere. Despite uncertainties in the exact solar zenith angle and the ground reflectivity, the data from this experiment indicated that roughly 1% of the solar flux incident on Venus at a solar zenith angle of about 85° is absorbed at the surface of the planet (Lacis 1975).

This experiment was followed by improved experiments on Venera 9 and 10 which measured upward as well as downward flux between 0.5 and 1.05 μm at 28 and 33° SZA (Moshkin et al. 1978), on Venera 11 and 12 (which included spectral measurements) at about 20° SZA (Moroz et al. 1980) and on Pioneer Venus at SZA 66° SZA in the wavelength range from 0.4 to 1.8 μm (Tomasko et al. 1980a). Near the surface, the measurements made by these various missions are relatively consistent with the expectations of forward scattering cloud models (Tomasko et al. 1980b) in showing greater penetrations of sunlight at small solar zenith angle (see Fig. 3). The measurements indicate that some 2.5% of the sunlight incident on Venus is absorbed at the surface of the planet (which would require a net radiative flux at thermal wavelengths of about 17 W m^{-2} over the entire planetary surface for thermal balance). While this is a small fraction of the sunlight incident at the top of the atmosphere, it is important in the thermal balance of Venus's lower atmosphere.

At visible wavelengths, the ground reflectivity is fairly low, less than 15%(Ekonomov et al. 1980) and at solar wavelengths the downward flux exceeds

the upward flux at the surface by a large factor, making net flux measurements relatively easy. At increasing altitudes, however, both upward and downward fluxes increase dramatically in a way that makes the net flux a moderately small fraction (15%) of either one by the time the cloud level is reached. In these circumstances, the measurement of net flux can be made most reliably if the same detector is used to measure the upward and downward flux. Such measurements were made on Venera 11 and 12, and are reported by Moroz et al. (1979; see also Chapter 19). The Venera 11 and 12 narrowband net flux profiles remain to be incorporated in a model that yields an estimate for the globally averaged bolometric net solar flux with altitude.

The Pioneer Venus Large probe measurements of net solar flux used different detectors for upward and downward flux measurements, but have been modeled to yield an estimate for the globally averaged bolometric net solar flux (Tomasko et al. 1980a,b). The resulting bounds on the solar net flux profile are given in Fig. 4. Above an altitude of 65 km where the probe measurements begin, a model calculation is shown.

The change in the net solar flux between any two levels indicates the amount of solar energy absorbed by the intervening layers of the atmosphere, which is available for heating these layers (see Sec. II). Roughly half of the solar energy absorbed by Venus is absorbed above the 64 km altitude where the Pioneer Venus Large Probe measurements began. This energy is absorbed in strong bands of CO_2 in the region near 1.6 and 2.0 um, and by the H_2SO_4 cloud particles which are essentially black longward of 2.5 um and have an optical depth of about 2 above 64 km altitude at this wavelength. In addition to the 35 W m^{-2} longward of 1 um, about 22 W m^{-2} are absorbed shortward of 0.5 um in the atmosphere above 64 km altitude, partly by SO_2 (shortward of 0.35 um) but mostly by an ultraviolet absorber which according to Toon and Turco (1982) might be amorphous sulphur. Between 64 and 57 km altitude, about 20 W m^{-2} are

absorbed of which ~15 W m^{-2} are absorbed shortward of 1 μm by the cloud particles and the remainder by weaker CO_2 bands longward of 1 μm. In the middle and lower cloud regions found between 57 and 48 km altitude, only an additional 8 W m^{-2} or so are absorbed. This is almost entirely due to CO_2 bands beyond 1 μm with a negligibly small amount absorbed by the cloud particles in this region (which have a visible optical depth of about 17). Between the cloud base at 48 km and about 40 km very little solar energy is absorbed. Between 40 and 15 km altitude an additional 15-20 W m^{-2} are absorbed, largely by an ultraviolet absorber shortward of 0.6 μm (suggested by Moroz to be a form of sulphur vapor) and partly by weak CO_2 and water bands longward of 0.7 μm. Little solar energy is absorbed in the lowest 15 km of the atmosphere. At the surface, some 17 W m^{-2} are absorbed.

C. Emission of Thermal Radiation

From the outside of the atmosphere, the total bolometric thermal emission can be measured rather directly. The measurements require integration over wavelength, emission angle, and longitude and latitude on the planet. The analysis of the measurements made by the Pioneer Venus orbiter Infrared radiometer (OIR) experiment give a total emitted flux of 157 $\pm$ 6 W m^{-2} (corresponding to effective temperature T_e = 229.4 $\pm$ 2.2 K) from measurements made in the northern hemisphere (Schofield and Taylor 1982c). Presumably the southern hemisphere would yield a similar value. For the whole planet to be in equilibrium with absorbed sunlight, the bolometric spherical albedo would have to be 0.76, which is in good agreement with Irvine's (1968) measured value of 0.77 $\pm$ 0.07. A value of 0.80 $\pm$ 0.02 was given by Taylor et al. (1980) in a preliminary interpretation of OIR data in a broad solar channel, but the uncertainty in this value may be larger than the value quoted due to calibration uncertainties (see Chapter 20 by Taylor et al.). Schofield and

Taylor (1982c) also give the thermal emission of Venus averaged in 10-deg wide bands of latitude. The emission is remarkably constant with latitude as already known from earlier work at a variety of wavelengths from Earth (see Tomasko et al. 1977). By contrast, the total amount of absorbed sunlight falls to zero at the poles somewhat more rapidly than the cosine of the latitude, μ_ℓ (roughly as $\mu_\ell^{1.4}$, Tomasko et al. 1980b) due to the increasing reflectivity of the forward scattering clouds at glancing incidence. The difference between the profile for the absorption of sunlight and the emission of thermal energy with latitude provides a basic drive for atmospheric dynamics.

The direct measurement of net thermal fluxes within the atmosphere is much more difficult than measurements from outside, and has only been attempted on the recent Pioneer Venus mission (Boese et al. 1979; Suomi et al. 1980). The measurements by the Large probe infrarer Radiometer (LIR) were seriously affected by a window misalignment at altitudes below 50 km, but seem reasonable above this altitude when the factor is removed from the caption of the figures in Boese et al. 1979 as revised by the author (Boese, private communication, 1982). In particular, the Large Probe thermal net fluxes are highly correlated with cloud structure measurements made on this probe, indicating the significant role of cloud thermal opacity (Boese et al. 1978).

The only thermal net flux measurements below the clouds are those made on the three PV small probes (Suomi et al. 1980). The instrument used a wide field of view and a wide spectral range (0.2 um to 150 um wavelength) to measure net flux. Two of the small probes entered in darkness, and measured thermal radiation only. The third (the "Day" probe) entered at a solar zenith angle of 79.9° and contains solar as well as thermal contributions. A model solar flux profile consistent with the Sounder probe solar flux measurements

has been used to generate the thermal flux profile shown in Fig. 4 for the Day Probe. For the other probes, the values as originally obtained by the experimenters are shown.

The thermal flux profiles are surprisingly variable from site to site in view of the great similarity in temperature profiles measured at these sites. In addition, at both the Night and North probe sites they are much greater than the globally averaged solar net flux profile at low altitudes, implying a substantial radiative imbalance in the lower atmosphere. In view of the large and variable nature of these flux measurements, the investigators have searched for instrumental problems which could have affected the measurements, and have found one that could have systematically increased the measured thermal net fluxes (Revercomb et al. 1982). The authors believe that they understand the vertical dependence of the flux errors, and by adjusting the fluxes to reasonable values at low altitudes, they have derived corrected thermal fluxes as shown in Fig. 5 (Revercomb et al. 1980). The fluxes of both the Day and Night probes (near latitude 30°S) are now in rough agreement with each other and with the solar net flux profile estimated to be typical of globally averaged conditions. The North probe thermal net flux profile is still somewhat larger than the others, but is consistent with model calculations.

It is important to be able to compute the net thermal radiative fluxes expected in Venus's lower atmosphere for the measured temperature profile. This requires knowledge of the composition and thermal opacity sources (see Eq. 4 in Sec. II) in the atmosphere. While CO_2 was long known to be an important constituent in Venus's atmosphere from its many absorption lines, the complexity of line formation in a scattering atmosphere prevented finding an accurate value for its mixing ratio until the entry of the Venera probes (Marov 1972). These measurements, together with the gas chromatograph

measurements on PV have indicated its mixing ratio to be $\sim$ 96.5% (Oyama et al. 1980b). Because this gas is the primary component of the Venus atmosphere and has a rich spectrum of vibration-rotation bands in the infrared, it is the dominant source of thermal opacity at many wavelengths. However, the net thermal flux depends most heavily on the opacity in spectral regions where the opacity is a minimum (between the bands) rather than in the strong bands. Furthermore, the total CO_2 abundance, pressure, and temperature of the lower atmosphere are so great that many weak transitions that are not observable under laboratory conditions are expected to occur. Thus it has been particularly difficult to obtain reliable information on the net thermal flux expected in certain spectral intervals (like, for example, the 3-4 um region) due to CO_2 opacity alone.

In the spectral intervals where CO_2 opacity is relatively small, the opacity of trace constituents can play an important role in determining the thermal opacity. Water vapor is potentially very important in this regard since it has strong absorptions in several CO_2 windows. Here the most important question has long concerned the water mixing ratio in the lower atmosphere. Earth-based spectroscopy has yielded water mixing ratios in the range from 10^{-4} to 10^{-6} (Belton 1969; Barker 1975) in the cloud-top region, though measurements on several Venera probes gave values of a few tenths of a percent (Morov 1972). However, if water makes up a part of the cloud particles, many types of direct sampling analyses may be prone to yield too high a value for the mixing ratio of the atmospheric water vapor due to contamination by water from cloud droplets. This is known to have happened during the PV mass spectrometer experiment when the inlet was actually plugged by a cloud droplet during a significant portion of the descent (Hoffman et al. 1980a) and may have contributed to the relatively high water mixing ratios (up to 0.5%) measured by the PV gas chromatograph experiment (Oyama et al. 1980b).

On the other hand, the optical spectrometer experiment on Venoras 11 and 12 would not be affected by this problem, and these data have been interpreted (Moroz et al. 1980a; see also Chapter 13) as indicating a local mixing ratio of water vapor which varies from about 2×10^{-4} in the region of the cloud bottom to about 2×10^{-5} near the surface. While smaller than some other estimates, these water vapor values are sufficiently large to provide an important source of thermal opacity in Venus's lower atmosphere (Pollack et al. 1980a).

Also observed in the lower atmosphere were SO_2 (at about 200 ppm) and CO (at about 20 ppm) (Oyama et al. 1980b), two gases which are significant sources of thermal opacity. Gases that have no allowed transitions in the infrared such as the noble gases provide negligible thermal opacity. Other gases such as HCl which may be present in mixing ratios of $\lesssim 1$ ppm are also ineffective thermal opacity sources.

In addition to the gases listed above, significant thermal opacity can be provided by the clouds covering the planet. The effectiveness of the cloud particles for blocking thermal radiation of a particular frequency depends on the composition of the particles (through the complex index of refraction) as well as the size distribution and the total mass of cloud material. Of particular interest is the opacity in the thermal infrared compared to that in the visible. This ratio is an important parameter in determining the effectiveness of the clouds in aiding the greenhouse effect.

Knowledge concerning the cloud structure is reviewed by Knollenberg et al. (1980) and by Esposito et al. (Chapter 16 in this book). Briefly, earth-based observations of the infrared spectrum by Pollack et al. (1974), and of the index of refraction of the cloud particles derived from polarization measurments by Coffeen (1968), Hansen and Hovenier (1974), Sill (1972), and Young and Young (1973) indicate that the clouds are composed of

strongly concentrated sulfuric acid (more than 70 % by weight) in the cloud-top region. The earth-based polarimetric measurements indicate that optical depth unity in the visible occurs at about the 50 mbar pressure level, and that the cloud particles are spherical with a narrow size dispersion about a mean effective radius of about 1 μm (Hansen and Hovenier 1974). The cloud particle size spectrometer (LCPS) on the PV Large probe made measurements of the size distribution and number density of the cloud particles at pressure levels from about 97 mbar (above which the visible cloud optical depth is roughly 4) to the surface. In addition to confirming the presence of the 1 μm radius size mode (termed mode 2), a distinct mode (mode 1) of smaller particles whose mean effective radius is about 0.5 μm was also seen. Both size modes were present in the three rather distinct cloud layers whose lower boundaries were at 49, 51, and 56 km altitude at the Large probe entry site. The mode 1 particles were seen in all three cloud layers as well as in an optically thin (at visible wavelengths) haze that extended below the main cloud layers to an altitude of about 30 km, and also above the main cloud layers.

In the middle and lower clouds, significant number densities of cloud particles up to 35 μm diameter (mode 3) were also seen. The presence of these larger particles is especially important for providing thermal opacity. If the sulfuric acid cloud particles have diameters of less than 3 μm, their absorption cross section at wavelengths longward of 10 μm will be nearly an order of magnitude smaller than their extinction cross section in the visible (see Fig. 6). Particles with diameter, d, greater than 6 or 7 μm, however, will have cross sections at thermal wavelengths which are generally within about a factor of 2 of their visible extinction cross sections. Thus, the mode 1 particles are quite ineffective in providing thermal opacity. The mode 2 particles ($d \sim 2$-3 um) with a total visible optical depth of about 11 can

provide a thermal optical depth in the order of unity. The mode 3 particles had a visible optical depth of about 5 at the Large probe site (Tomasko et al. 1980a) and can provide thermal optical depths of 2 to 3, but only within the middle and lower clouds where they are found.

The above estimates for the thermal opacity of the mode 3 particles use Fig. 5 and thus assume the particles are composed of concentrated sulfuric acid. There has been some question about the validity of this assumption arising from the fact that the PV nephelometer measurements of back scattered light, as well as the observed rate of decrease of upward and downward flux through the middle and especially the lower cloud, are not in agreement with the expected values calculated by assuming all the cloud particles measured by the LCPS experiment are spherical sulfuric acid droplets. Essentially no disagreement is seen in the upper cloud where no mode 3 particles are observed by the LCPS. The LCPS investigators have suggested that the problems can be resolved if the mode 3 particles are elongated crystals rather than spheres, and cite some features in their raw data to support this suggestion (Knollenberg and Hunten 1980). However, no completely satisfactory composition has yet been suggested for the solid cloud material.

Recently, Toon and Blamont (1982) have suggested that the mode 3 particles may not be a separate size mode but simply an extended tail of the mode 2 sulfuric acid spheres which reaches to quite large sizes. These authors suggest that a slight miscalibration of one size range in the LCPS instrument may have led to the impression that these particles formed a separate size mode. If this interpretation proves correct, the composition of the largest particles would be sulfuric acid, and the visible optical depths deduced from the Large probe solar flux radiometer (LSFR) experiment could safely be converted to thermal opacities along the lines outlined above.

One other possibly important source of thermal opacity was suggested by

Suomi et al. (1980). If aerosol particles are sufficiently small for a given real refractive index, their scattering cross section can be made small in the visible as well as in the infrared. However, their absorption optical depth is separately determined by their imaginary index of refraction and the mass of aerosol per unit surface area in the clouds. For sulfuric acid, the imaginary index is large in the infrared and near zero in the visible. Thus it is possible to adjust the aerosol mass per unit area to achieve any desired absorption optical depth in the infrared, and to choose a sufficiently small particle size to make the scattering optical depth negligibly small at wavelengths longer than any specified wavelength in the visible. Therefoere the particles might not have been seen by the LSFR experiment which is sensitive in the visible, or by the LCPS experiment, because the particles were too small, but they could still provide an important contribution to the thermal opacity.

One motivation for suggesting the presence of these particles is the fact that the orbiter infrared (OIR) instrument on PV measured brightness temperatures near 11 μm (where gaseous opacity is a minimum) which implied that over much of the planet an aerosol optical depth of unity at 11 μm is reached at a pressure of about 100 mbar (Schofield and Taylor 198?). At 0.63 μm in the visible, the LSFR data (Tomasko et al. 1980a) suggest that the aerosol optical depth above the 100 mbar level is about 4. By extrapolating the measured LCPS partition between mode 1 and 2 type particles to higher altitudes, these authors assumed that the optical depth in the visible above the 100 mbar level would be about 2.3 due to mode 2 and about 1.7 due to mode 1. The corresponding absorption optical depth at 11 μm would be only about 0.1 for mode 1 and about 0.5 for mode 2, approximately half the value required by the OIR measurements. The proposed mode of submicron particles (dubbed mode 0) could be responsible for the rest.

However, the partition between modes 1 and 2 between 97 mbar (where the visible optical depth is 4) and $\sim$ 40 mbar (where the visible optical depth is 1) is rather uncertain because neither the orbiter nor probe experiments measured this region well. If nearly all (instead of 1/2) of the visible optical depth in this region were caused by mode 2 particles, the 11 μm aerosol optical depth above 100 mbar would be nearly 1 as observed. Thus the need for a significant population of mode 0 particles is questionable.

Further it is worth noting that the mode 1 particles in models E and F in Tomasko et al. (1980) were mislabeled as being H_2SO_4 when in fact their optical properties were computed using a real refractive index of 1.93 (more appropriate for sulfur). Thus, the value of the scaling factor (1-g) which should be used to scale the mode 1 particles optical depths to effective isotropic optical depths really is 0.515 rather than 0.265 as given in Table 6 and shown in Fig. 12. That is, the entries in the second column of Table 6 giving the effective isotropic optical thickness of the mode 1 particles in each layer of model F should be nearly twice as large as shown. Even if only half the optical thickness of mode 1 particles between 38 and 97 mbar in model F were replaced by an equivalent amount of mode 2 particles, the thermal opacity of the clouds above 100 mbar would nearly double without changing the visible opacity of the clouds or adding mode 0. Despite this labeling error, none of the other conclusions of Tomasko et al. (1980) particularly concerning the scaling of the measured solar flux profile to globally averaged conditions or to include wavelengths outside the LSFR bandpass, are affected. Indeed, model F provides some support for the work of Toon and Turco (1982) who suggest that amorphous sulfur may be the ultraviolet absorber, and Toon et al. (1982) who require a component with a high refractive index to explain the PV nephelometer results in the upper cloud. It now seems also that the particle number densities measured by the LCPS in the upper cloud do not provide

sufficient visible optical depth to be consistent with the decrease in the solar flux through this cloud unless a component with a high refractive index is present.

The horizontal variability in the thermal opacity produced by the clouds is difficult to estimate. The OIR measurements indicate that aerosol optical depth unity is reached at about the same pressure level ($\sim$100 mbar) except in the polar regions. Also, there are strong similarities in the visible cloud structure as revealed by the PV nephelometers and the Venera and PV solar flux profiles over much of the planet. On the other hand, the thickness of the lower cloud (which contained the greatest contribution of the mode 3 particles at the Large probe site) appears to be rather different at the 4 PV probe sites in the nephelometer data. Also, the thermal net flux measurements in the clouds made by the Small probe net flux radiometer (SNFR) instruments are quite different at the three small probe entry sites. Nevertheless, in view of the relative uniformity of the planet in the thermal infrared, the thermal opacity of at least the upper portions of the clouds vary relatively little over most of the planet.

D. Wind Field

The winds in the lower atmosphere have been measured by the differential long baseline interferometry (DLBI) experiment on the 4 PV probes (Counselman et al. 1980), and also on the Venera 8 through 12 probes (Marov et al. 1973a; Antsibor et al. 1976; Kerzhanovich et al. 1979b). Figure 7a from Schubert et al. (1980a) summarizes the zonal wind profiles measured below the clouds. The PV measurements for the Day and Night probes, which landed at nearly equal latitudes near 30°S, are almost identical and are shown as a single curve. The zonal winds are westward at all altitudes. High velocities of nearly 100 m sec^{-1}, are measured at cloud-top altitudes decreasing to 1 m sec^{-1} or less

(about the measurement uncertainty) at altitudes below about 7 km. Below about 30 km altitude the zonal wind speed decreases with increasing latitude. Many of the profiles show alternating layers of high and low wind shear. Measurements using anemometers on Veneras 9 and 10 while on the surface gave wind speeds of 0.3 to 1 m sec^{-1}, consistent with these results (Avduevskii et al. 1976b).

Figure 7b shows the DLBI measurements of meridional winds from the 4 PV probes (Counselman et al. 1980); the data show the noise level ($\sim$0.5 m sec^{-1}) superimposed on a complex structure. In the lowest 30 km the meridional velocities are quite small but seem to show significant variations which may be indicative of eddy motions (Schubert et al. 1980a). The small meridional motions (comparable to the measurement uncertainties) make it impossible to determine whether or not a mean Hadley cell exists at these atmospheric levels, or to estimate the meridional heat transport due to such a cell or to the eddies.

While the meridional winds vary significantly in magnitude and direction at altitudes above 40 km, they are equatorward on all 4 PV probes at altitudes between about 50 and 55 km. Near the cloud tops (65-70 km altitude) the winds measured by tracking ultraviolet cloud features (Rossow et al. 1980a) give small ($\sim$ 10 m sec^{-1}) meridional motions directed toward the poles in each hemisphere. Taken together, these measurements imply the existence of a weak Hadley cell superimposed on the strong zonal winds operating at cloud levels. Since most of the solar radiation absorbed by Venus is absorbed at cloud levels and above, the ability of this Hadley cell to transport heat poleward can be expected to be important in limiting the equator-to-pole temperature contrasts to the modest values observed at these altitudes.

E. Other Processes

Several other processes have been suggested from time to time as contributing in important ways to the thermal balance of Venus's lower atmosphere. For example, it has been suggested that wind blown dust could cause significant thermal opacity or possibly even contribute to heating the surface through frictional effects (Opik 1961). The observed virtual absence of aerosols in the lowest 30 km of the atmosphere by the PV nephelometer and LCPS experiments indicates that these effects are negligibly small.

Heat generated by radioactive decay in the interior of the planet has also been suggested as an important energy source for the lower atmosphere (Hansen and Matsushima 1967). However, current estimates (Toksoz et al. 1978) place the flux of internal heat for Venus about 2 orders of magnitude less than the solar flux that has been measured to reach the surface.

One potentially important heat transfer process involves the vertical transport due to heats of formation and latent heat release during the vertical cycling of cloud vapor. Assuming that all the particles measured by the LCPS are spherical led Knollenberg and Hunten (1979) to estimate an upward heat flux of 8 W m^{-2} for this effect, about 20% of the globally averaged downward net solar flux at cloud levels. However, most of the cloud mass was contained in the mode 3 particles, and the assumption that these particles are spherical leads to problems in the interpretation of the nephelometer and solar flux measurements. If the mode 3 particles are irregularly shaped crystals, the total cloud mass could be as much as a factor of 2 less, with the heat flux decreased at least proportionally. The recent interpretation of the mode 3 particles as a large particle tail of mode 2 presumbably would also lead to some reduction of this heat flux estimate, but probably by a smaller factor that remains still to be calculated. In any case, this heat transfer process is probably significant for Venus but at a level comparable to current

uncertainties (~20%) in the solar net flux at cloud levels.

II. Models of the Thermal Balance

A. General Framework

In a steady state, the algebraic sum of the rates of heating and cooling of the atmosphere due to the total of all physical processes should add to zero at each location. At a given location, the heating and cooling rates depend on the state of the atmosphere - its temperature, pressure, composition, radiation and wind fields. A successful steady-state model for the thermal balance of Venus's lower atmosphere will include the relationships of the heating and cooling rates to the atmospheric state and show that the atmospheric structure that leads to no net heating or cooling at each location is equal to the observed structure.

For radiative processes, these rates are defined and related to the atmospheric structure as follows. Let the diffuse intensity of radiation at altitude z in the atmosphere,

$$I(z, \lambda, \theta, \varphi) = dE/(dt,\ dA_\perp\, d\Omega\, d\lambda), \qquad (1)$$

be defined as the rate at which radiant energy dE between wavelength limits λ and $\lambda + d\lambda$ traveling within a differential cone of solid angle $d\Omega$ about the direction specified by zenith and azimuth angles θ and φ respectively crosses a unit area $dA_\perp$ oriented perpendicular to the direction of the beam. The units of I are, for example, watts m^{-2} $ster^{-1}$ um^{-1}. The net rate at which sunlight of wavelength crosses a horizontal surface of unit area at altitude z is given by the net flux, $F_n(\lambda, z)$, evaluated by integrating over solid angle -

$$F_n(\lambda,Z) = \int_0^{\pi}\int_0^{2\pi} I(\lambda,Z,\theta,\varphi)\cos\theta\,\sin\theta\; d\varphi d\theta + \cos\theta_o\, F_o\, e^{-\tau(\lambda, Z, \theta_o)} \qquad (2)$$

Here the cos θ projection factors in each term convert $I(\theta)$, the energy per

unit area perpendicular to each beam direction, to the energy per unit area of horizontal surface. The second term represents the reduced incident solar flux which survives to altitude z without being absorbed or scattered into the diffuse intensity field. Notice that when $I(\theta=0)$ represents intensity traveling upward, this equation gives the net solar flux (which is directed downward) as negative. (With this convention, θ_0, the zenith angle toward which the incident solar flux is traveling, is $\theta_s + \pi$ where θ_s is the local zenith angle of the sun.)

The magnitude of the net solar flux at any altitude is the amount of solar energy absorbed below that altitude. The difference in the net flux at any two levels is the amount of energy absorbed by the intervening layer of atmosphere and available for heating the layer. Thus, when the atmosphere can be approximated by plane parallel layers (such as when the thickness of the atmosphere is much less than the planetary radius), the radiative heating rate $\mathcal{H}(z,\lambda)$ at the altitude z for radiation of wavelength λ is given by

$$\mathcal{H}(z,\lambda) = -\frac{1}{\rho(z) c_p} \frac{d F_n(z,\lambda)}{dz} \qquad (3)$$

where $\rho(z)$ is the local atmospheric density and c_p is the specific heat capacity per unit mass at constant pressure, and depends on the atmospheric composition. The local solar heating rate in addition depends strongly on longitude and latitude through its dependence on the zenith angle of the sun.

In addition to being heated by absorbing sunlight, the atmosphere can be cooled (or heated) be emitting and absorbing thermal radiation. Here the upward and downward intensities of thermal radiation at altitude z are given by

$$I(z,\lambda,\theta) = \int_0^z B[T(z'),\lambda] \exp\{-[\tau(z',\lambda,\theta) - \tau(z,\lambda,\theta)]\} \, d[\tau(z',\lambda,\theta)] \qquad (4)$$
$$+ I_s(z=0,\theta,\lambda) \exp\{-[\tau(0,\lambda,\theta)] - \tau[z,\lambda,\theta]\}$$

for $0 \le \theta < \pi/2$

and

$$I(z,\lambda,\theta) = \int_z^\infty B[T(z',\lambda)] \exp\{-[\tau(z,\lambda,\theta) - \tau(z',\lambda,\theta)]\} d[\tau(z',\lambda,\theta)]$$

for $\pi/2 \leq \theta < \pi$.

The upward intensity includes a term representing the contribution of the emission from the planet's surface which survives to altitude z. Here B[T(z, λ)] is the Planck function which gives the thermal emission of a black body at temperature T at wavelength λ. Note that the optical depth τ at wavelength λ depends on the slant path through the gas at zenith angle θ. In the thermal infrared, special techniques are often required to deal with the rapid variation of the opacity of the gases with wavelength (see Pollack 1969).

The net thermal flux is given by integration over solid angle as in Eq. 2 except that I is independent of azimuth angle and the second term which represented the reduced solar flux is omitted at thermal wavelengths. Positive net thermal flux is directed upward, and the local cooling rate due to any increase of net thermal flux with increasing altitude is given by

$$\Lambda(z,\lambda) = \frac{1}{\rho(z)\, c_p} \frac{d F_n(z,\lambda)}{dz} . \qquad (5)$$

This function can also vary with longitude and latitude due to changes in opacity sources (clouds or trace constituents) or to changes in the temperature structure of the atmosphere.

In principle, if the temperature and pressure structure and the composition of the atmosphere are known, the optical depth between any two levels can be calculated at each wavelength, and the thermal radiation field, net flux, and local radiative cooling rate can be computed from Eqs. 4 and 5. Of course, the opacity due to the aerosols must be included also. Likewise,

if the optical properties and spatial distribution of the aerosols are known in sufficient detail, the solar radiation field can be obtained by solving the equation of radiative transfer including multiple scattering (see, for example, Chandrasekhar 1960), and the solar net flux profile and heating rate follow from Eqs. 2 and 3. In practice, the comparison of measured and computed flux profiles are useful for providing checks on the gaseous composition and the distribution and nature of the aerosols.

At any location on the planet, the difference from zero of the sum of the radiative solar heating and thermal cooling rates, integrated over all wavelengths and for an appropriate length of time, must be balanced by other processes (such as atmospheric dynamics) to yield a long-term steady state. Because of the difficulties of correctly including a three-dimensional treatment of atmospheric dynamics, some extreme simplifications are commonly made. For example, the problem can be reduced to one dimension by simply assuming that horizontal motions cause the globally averaged heating and cooling rates to balance at each altitude. By iterative techniques, it is possible to find a temperature-pressure structure for the given composition and cloud properties for which the globally averaged radiative heating and cooling rates balance. This temperature structure is then tested for stability against convective overturning by comparing the temperature gradient in the model with the adiabatic temperature gradient. Wherever the magnitude of the model temperature gradient exceeds the magnitude of the adiabatic gradient, convection is assumed to occur, and the temperature profile of the model in radiative equilibrium is replaced by the adiabatic profile. Because of the efficiency of atmospheric convection, it is assumed that the temperature gradient needs to be only very slightly superadiabatic for convective transport to make up for the excess of the solar heating over the radiative thermal cooling rate (see, for example, Goody and Walker).

Despite their simplicity, such one-dimensional radiative-convective models have played an important role in the development of theories of the thermal balance of the lower atmosphere of Venus as shown in the next section. As indicated in the final section, their extension to include a more realistic treatment of atmospheric dynamics remains a significant challenge for the future.

B. Historical Developments

Advance beyond the "Earth's twin" notion of the Venus atmosphere, and the beginning of attempts to understand the state of Venus' atmosphere date from the discovery of the high brightness temperature of Venus at centimeter wavelengths (Mayer et al. 1958). Early attempts to explain these observations were hampered by the general uncertainty regarding the state of Venus's lower atmosphere including its composition, surface pressure, and cloud structure, and ranged widely - from nonthermal ionospheric emissions to heating by wind blown dust (Opik 1961) to greenhouse models driven by internal heat or absorbed sunlight (Sagan 1960). With the Mariner 5 and Venera 4 missions (in October 1967) the surface temperature and pressure as well as the high mixing ratio of carbon dioxide were clearly established, removing any doubt that the high microwave brightness temperatures were due to thermal emission from the hot surface of the planet. Still, several possible explanations of the hot lower atmosphere remained. Because the effective temperature seen from outside the atmosphere was nearly 500 K lower than the surface temperature, it was clear that the thermal opacity of the atmosphere must be great. Debate concerned how to achieve the required large thermal opacity without violating spectroscopic, microwave, or Venera spacecraft constraints on the amount of water present. Clouds could always be assumed to provide a large thermal opacity, but the thicker the clouds were made in the infrared, the thicker

they were in the visible and the less sunlight would penetrate to the surface.

After the Venera 4 and Mariner 5 flights, Pollack (1969) used non-gray calculations to show that a composition consistent with available constraints (90% CO_2, 10% N_2, 0.5% H_2O) and a cloud of optical thickness $\sim$20-40 in the visible (corresponding to $\sim$3 times less in the thermal infrared) would provide sufficient thermal opacity to give the measured effective temperature for the observed temperature structure. By equally significant calculations, Pollack generated models of the penetration of solar energy through these clouds (assumed to be composed to water spheres) and showed that sufficient sunlight would penetrate and be absorbed beneath the clouds to maintain the high surface temperature.

Nevertheless, the water vapor abundance measured from the Earth was too low to be consistent with clouds composed of water or ice; the composition of the clouds therefore still was unknown (the properties of dust clouds were being actively pursued [Samuelson 1967]), and no firm information on the optical thickness of the clouds in the visible was available. It was still unclear whether the actual cloud structure resembled Pollack's model and whether sufficient sunlight could penetrate the actual clouds to replace even the small amount of thermal flux which was seen to be leaking out. If sufficient sunlight did not reach the surface, it was suggested that very large amounts of dust in the atmosphere (Hansen and Matasushima 1967) might provide an extremely large amount of atmospheric thermal opacity such that the small amount of heating due to radioactive decay in the planet's interior could replace the small escaping thermal flux and support the hot lower atmosphere. But again, the mechanism for raising the dust (particularly after the dust became thick enough to prevent sunlight from heating the lower atmosphere) remained unclear.

At about this time, Goody and Robinson (1966) considered the possibility

that the nonuniform solar heating over the planet could cause a deep circulation of the atmosphere even if all the solar heating occurred at cloud levels and none penetrated to the ground. They suggested that the difference in heat input between the subsolar and antisolar points would result in a narrow descending column of atmosphere near the antisolar point and slowly rising motions over the rest of the globe. Using the Boussinesq approximation (neglecting density variations except for buoyancy terms) they found the circulation would penetrate essentially to the surface and cause an adiabatic temperature gradient throughout the lower atmosphere and a high surface temperature.

The ability of this indirect circulation to lead to an adiabatic profile in the atmosphere was soon questioned by other authors (e.g. Hess 1968). Stone (1975) pointed out that the thermal time constant for the lower atmosphere was sufficiently large so that even for the slow rotation period of Venus, the diurnal temperature difference expected was negligibly small. Thus, the Goody and Robinson circulation would be expected to occur between the equator and the poles rather than the subsolar and antisolar points. Numerical calculations by Kalnay de Rivas (1975) showed that the Goody and Robinson circulation did indeed occur also when she used the Boussinesq approximation. However, when she included the effects of the variation of density (by about a factor of 100) between the surface and the cloud levels, the circulation did not penetrate more than a few km ($\sim$ a scale height) below the levels where the solar heating occurred. The lower atmosphere remained at rest and followed an isothermal, not an adiabatic, temperature profile. She concluded that penetration of sunlight to low levels (or some other deep heat source) was required to explain the observed vertical temperature structure of the lower atmosphere.

Of course, even with the deep penetration of sufficient sunlight, mass

motions would be required to transport heat meridionally to give the relatively small latitudinal thermal contrasts observed in the face of the large variation in solar heating with latitude. The long thermal time constant of the lower atmosphere which could smooth diurnal effects would not suppress latitudinal temperature differences without atmospheric dynamics, but with deep penetration of sunlight to provide a drive for the circulation, a variety of types of circulation from eddies to a smooth Hadley cell could be conceived which might provide the transport.

C. Recent Models

By the time of the Venera 8 entry probe to Venus, sulfuric acid had been identified as an important constituent of the clouds of Venus (Young and Young 1973; Sill 1972; and Pollack et al. 1974). Nevertheless, among the great uncertainties in understanding the thermal balance of Venus's lower atmosphere was the unknown thickness and optical properties of the clouds which would control the penetration of solar energy. The Venera 8 measurements showed for the first time that a significant amount of sunlight penetrated to the surface of the planet. Also, they indicated that the clouds extended down to an altitude of $\sim$35 km at the Venera 8 entry site, occupying a substantial vertical extent of the atmosphere below their tops at $\sim$ 70 km altitude. For the first time, solar deposition profiles could be calculated for comparison with direct observations.

Pollack and Young computed globally averaged, one-dimensional radiative-convective equilibrium models, subject to the new observational constraints; the H_2O vapor pressure was taken to be that in equilibrium with concentrated sulfuric acid cloud particles in the cloud (and 0.3% below them), and the cloud optical depths were consistent with the Venera downward visible flux measurements. The results of greatly decreasing the water vapor abundance in

the altitudes above 35 km suggested that the thermal opacity of the cloud particles would have to play an important role for the greenhouse to work. When 3 um radius droplets were used instead of the 1 um radius droplets deduced from polarimetry of the cloud-top region, the radiative temperature profile became steeper than the adiabatic profile at about the 15 bar pressure level, leading to a high surface temperature, though not quite as high as the observed level. The authors felt that sufficient uncertainty still existed regarding several atmospheric parameters and that reasonable adjustments could allow the model to produce essentially the observed high surface temperature. For example, useful as the Venera 8 optical measurements were, they measured only downward flux and did not uniquely determine the visible cloud optical depths. Also, uncertainties in the particle size distribution deep in the clouds still produced large uncertainties in the thermal opacity of the clouds. (See Tomasko et al. [1977,1979b] for a review of the uncertainties concerning the thermal balance of the Venus atmosphere at this time.)

Many of these uncertainties have been considerably reduced by the Venera 9-12 and Pioneer Venus missions. Data from the nephelometers, upward and downward viewing optical radiometers, and the cloud particle size spectrometer have indicated the global similarities in the cloud structure with a well defined lower boundary at 48 km altitude from measurements at 8 additional entry sites. The particle size distributions have been precisely measured at one site and strongly constrained by the nephelometers at all the sites. The net solar flux profile has been measured at several sites, and some estimates of the globally averaged profile are beginning to appear. Measurements of the water vapor abundance beneath the clouds have been made in a way that is not susceptible to contamination by the liquid water content of the cloud droplets. Direct measurements of the abundance of trace constituents which can also provide thermal opacity (such as SO_2) have been

made in the lower atmosphere by several techniques. Equally important, very accurate profiles of the temperature and thus the static stability have also been determined at several sites.

One-dimensional globally averaged radiative-convective models have been computed incorporating these new observational constraints. Even in the presence of some simplifying assumptions, early calculations (Tomasko et al. 1979) showed that the stably stratified layer observed under clouds (from about 30 to 50 km altitude) and the high surface temperature could be reproduced by models incorporating the solar net flux profile and the Venera water vapor mixing ratio ($\sim 2 \times 10^{-4}$). When a water vapor mixing ratio larger by a factor of 10 was used below the clouds, the profile became adiabatic in the clouds and remained so to the ground.

Calculations have been made by Pollack et al. (1980a) that include opacity due to SO_2, CO, HCl, as well as some additional pressure-induced transitions in CO_2. The water vapor mixing ratio in their base case varied from 2×10^{-5} at the surface to 2×10^{-4} in the clouds before rapidly decreasing to 2×10^{-6} at the cloud tops. Models with the nominal and high solar net flux profile from PV and the Venera 11 water profile yield surface temperatures of 720 K and 760 K, bracketing the observed surface temperature of 730 K (see Fig. 8). Furthermore, these models contain an extended stable layer beneath the clouds and have static stability profiles qualitatively similar to the observed profiles (Fig. 9). When a water vapor mixing ratio corresponding to the PV gas chromatograph measurements (about a factor 50 greater) is used, this stable layer disappears from the model and the surface temperature increases to about 820 K (nearly 100 K higher than observed).

In the base case model, the second stable region observed between 15 and 20 km altitude does not form, but the authors point out that the shift of the blackbody curve to shorter wavelengths at the high atmospheric temperatures in

the lowest 30 km leads to an increase in the net thermal flux due to a relative window in the 2.1 to 2.6 μm region. As a result, the net thermal radiative flux carried by the adiabatic profile is nearly as large as the solar net flux. Small changes in the model might lead to the reappearance of a stable region at low altitudes.

Considering the simplifications inherent in a one-dimensional radiative-convective model, the agreement with the observed temperature profiles is remarkable. Nevertheless, significant uncertainties remain even in these simplified models. For example, the total thermal flux emerging from the top of the model can exceed the observed flux by a large factor (nearly 1/3) when the nominal cloud model is used and no mode 0 aerosols are added. If sufficient mass ($\sim$0.1 mg cm^{-2}) of mode 0 aerosols is included above the middle cloud to provide the required thermal opacity ($\sim$1 at 10 μm), the diameter of these particles must be less than about 0.07 μm to give less than a scattering optical depth of unity near 0.32 um in the ultraviolet (Tomasko et al. 1980b). Their number density would be about 2 x 10^5 cm^{-3} if they were distributed over a 30 km range of altitudes above 57 km. The time for coagulation to remove these particles (convert them to significantly larger sizes) would be several hours. It remains to be seen whether mechanisms can be proposed to replace this aerosol mass in an equally short time. On the other hand, it may be that the optical depth of mode 2 particles has been underestimated in the nominal cloud model (as suggested in Sec. I) in a way that might provide the bulk of the missing opacity by the mode 2 particles alone. Interestingly enough, Pollack et al. (1980a), remark that the existence and nature of the stable layer found just beneath the clouds in their models depends on the amount and distribution of the mode 0 absorbers. The infrared opacity of the clouds apparently is still a matter for further investigation.

Also somewhat unsettled is the treatment of the thermal opacity produced by the gases in the high temperature, high pressure lower atmosphere of Venus. Pollack et al. (1980a) show much of the thermal flux at altitudes of 30 km or less being carried at rather short wavelengths (less than 3 μm). While these authors relied in part on theoretical calculations in an attempt to include a fairly complete set of transitions, numerous transitions arising from excited states (hot bands) and from very weak overtone and combination bands, undoubtedly occur in this spectral region, even though they have not yet been observed in the laboratory. Thus, it is difficult to be sure of the completeness and accuracy of the gaseous opacities used in the model computations.

If the gaseous opacities are inaccurate, they are probably somewhat too low due to the limited number of transitions included, rather than too high. Thus, while the measured thermal net fluxes might well have been a bit lower than computed fluxes, it is quite surprising to find the first measured thermal fluxes significantly greater than the computed fluxes in the lower atmosphere. The "corrected" measured fluxes at low latitudes given by Revercomb et al. (1982) are now in agreement with fluxes computed using water abundances in the range of values measured at low latitudes by the Venera 11 and 12 probes. If it were available, a separate measurement of lower water abundance at high latitudes, as suggested by the revised North probe flux profile (see Fig. 5), would be an important confirmation of both the revised flux profiles and the opacity tables currently in use.

It could be argued that since the thermal net flux produced by the adiabatic temperature profile is close to the solar net flux in the models and a slightly stable region is seen in the lowest portions of the PV descent profiles, the thermal gaseous opacities are close to correct in the models. Small adjustments, for example, in the average solar flux profile or even a

slight decrease in the thermal opacities would produce a marginally stable temperature profile as observed at low altitude (at about 15 km). However, no effects due to global circulation have yet been included in the model other than assuming that horizontal motions distribute the heat as required to produce the small horizontal contrasts observed. On Earth, global circulation (aided by latent heat effects) produces a mean lapse rate that is only 2/3 of the adiabatic value despite the presence of convection (Stone 1975). It may be unreasonable to expect the one dimensional models to reproduce all the features in the vertical temperature profile.

In this regard we should comment briefly on the state of including the dynamics in a comprehensive picture of the thermal balance of Venus's lower atmosphere. (For a more complete discussion, the reader is referred to Schubert et al. [1980a] and chapter 21 in this book by Schubert.) As outlined by Stone (1975), comparison of the radiative and dynamical time constants as functions of height in the atmosphere can be instructive. He points out that below ~ 56 km altitude, the dynamical time constant is much less than the radiative time constant, and the dynamics are expected to determine the thermal structure of the atmosphere. He also points out that the radiative time constant is greater even than the length of one Venus day, so that the thermal inertia of Venus's lower atmosphere is sufficient to eliminate diurnal temperature variations even without zonal winds. Meridional heat transport by mass motions would be expected to occur, and should be driven by the strong latitudinal variations in solar heating. These motions could take the form of a slow Hadley cell with rising motions at the equator, flow toward the poles, and a deeper slow return flow. Substantial heat flux rates can be carried by even very slow motions in the lower atmosphere due to the great density; the predicted wind speeds near the surface are ≤ 1 m sec^{-1}. Eddy motions could also transport the heat. Stone points out, though, that a Hadley type

circulation transports heat poleward only if the poleward branch is at a higher potential temperature than the equatorward return flow at lower levels. In other words, this type of motion transports heat poleward only if the temperature gradient is slightly subadiabatic. It seems possible that improvements in the thermal opacity tables for the lower Venus atmosphere will increase the opacity and make the one-dimensional models no closer to the slightly stable measured temperature profile. The details of the modifications to the temperature field caused by the dynamics will have to await a successful global circulation model, but such modifications could conceivably be responsible for the low altitude stable layer observed.

Substantial work remains to be done before the global circulation is modeled, despite the great body of observational data recently collected. For example, many features of the wind field measured for Venus are qualitatively as expected, including the low wind speeds observed at depth, and the direction and magnitude of meridional flows in the clouds. However, the most striking feature of the circulation remains the rapid zonal flow ($\sim$100 m sec^{-1}) near the cloud tops. This dramatic aspect of the flow still remains to be understood and reproduced in a detailed calculation.

In summary, instruments on entry probes have now measured many of the properties of the lower atmosphere of Venus which control the transfer of solar and thermal radiation. One-dimensional radiative-convective models indicate that sufficient sunlight penetrates to low levels and is trapped by the large infrared opacity of the atmosphere to yield essentially the high temperatures observed. Nevertheless, several features in the temperature structure, such as the relatively small latitudinal contrasts and the existence of a deep stable region, indicate that atmospheric motions also play an important role. While we know that atmospheric dynamics is responsible for some of these effects, the complexities of the processes are such that they

have yet to be modeled successfully in detail.

Acknowledgments

It is a pleasure to acknowledge the benefit of many enlightening discussions with numerous colleagues from the Pioneer Venus community during the course of my participation in that program. This work has been supported by a grant from the National Aeronautics and Space Administration.

REFERENCES

Antsibor, N. M., Bakit'ko, R. V., Ginzburg, A. L., Gudiyakov, V. T., Kerzhanovich, V. V., Makarov, Yu. F., Marov, M. Ya., Molotov, E. P., Rogal'skii, V. I., Rozhdestvenskii, M. K., Sopokin, V. P. and Shnzgin, Yu. N. 1976. Estimates of wind velocity and of instruments dropped from Venera 9 and Venera 10. Cosmic Research, 14:625-631.

Avduevsky, V. S., Marov, M. Ya., Moskin, B. E., and Ekonomov, A. P. 1973. Measurement of solar illumination through the atmosphere of Venus. J. Atmos. Sci. 30: 1215-1218.

Avduevskii, F. S., Vishnevetskii, S. L., Golov, I. A., Karpeishkii, Yu. Ya, Lavrov, A. D., Likhushin, V. Ya., Marov, M. Ya., Mel'nikov, D. A., Pomagin, N. I., Pronina, N. N., Razin, K.A., and Fokin, V. G. Measurement of Wind Velocity on the Surface of Venus During the Operation of Stations Venera 9 and Venera 10. Cosmic Res. 14:622-625.

Barker, E. S. 1975. Comparison of simultaneous CO_2 and H_2O observations of Venus. J. Atmos. Sci. 32: 1071-1075.

Barker, E. S. 197 . Observations of Venus water vapor over the disk of Venus: The 1972--74 data using the H_2O lines at 8197 A and 8176 A. Icarus.

Belton, M.J.S. 1969. Theory of the curve of growth and phase effects in a cloudy atmosphere: Applications to Venus. In The Venus Atmosphere, eds. R. Jastrow and S. I. Rasool (New York: Gordon and Breach), pp. 283-322.

Boese, R. W., Pollack, J. B., and Silvaggio, P. M. 1979. First results of the large probe infrared radiometer experiment. Science. 203: 797-800.

Coffeen, D. L. 1969. Wavelength dependence of polarization. XVI. Atmosphere of Venus. Astron. J. 74: 446-460.

Councilman III, C. C., Gourevitch, S. A., King, R. W., Loriot, G. B., and Ginsburg, E. S. 1980. Zonal and meriodinal circulation of the lower atmosphere of Venus determined by radio interferometry. J. Geophys. Res.

85:8026-8030.

Ekonomov, A. P., Golovin, Yu. M., and Moshkin, B. E. 1980. Visible radiation observed near the surface of Venus: Results and their interpretation. Icarus 41:65-75.

Goody, R. M. and Robinson, A. R. 1966. A discussion of the deep circulation of the atmosphere of Venus. Astrophys. J. 146:339-355.

Hansen, J. E., and Hovenier, J. W. 1974. Interpretation of the polarization of Venus. J. Atmos. Sci. 31:1137-1160.

Hansen, J. E. and Matsushima, S. 1967. The atmosphere and surface temperature of Venus: A dust insulation model. Astrophys. J. 150:1139-1157.

Hess, S. L. 1968. The hydrodynamics of Mars and Venus. In The Atmospheres of Mars and Venus, eds. J. C. Brandt and M.B. McElroy (New York: Gordon and Breach) pp. 109-131.

Hoffman, J. H., Oyama, V. I., and von Zahn, U. 1980. Measurements of the Venus lower atmosphere composition: A comparison of results. J. Geophys. Res. 85:7871-7881.

Irvine, W. M. 1968. Monochromatic Phase Curves and Albedo for Venus. J. Atmos. Sci. 25:610-616.

Kalnay de Rivas, E. 1975. Further numerical calculations of the circulation of the atmosphere of Venus. J. Atmos. Sci. 32:1017-1024.

Kerzhanovich, V. V., Markarov, Yu. F., Marov, M. Ya., Kozhdestvensky, M.K., and Sorokin, V. P. 1979. Venera 11 and Venera 12: Preliminary estimates for the wind speed and turbulence in the atmosphere of Venus. NASA Tech. Note N80-23240.

Knollenberg, R. G. and Hunten, D. M. 1979. Clouds of Venus: A Preliminary Assessment of Microstructure. Science, 205:70-74.

Knollenberg, R. G. and Hunten, D. M. 1980. The Microphysics of the Clouds of Venus: Results of the Pioneer Venus Particle Size Spectrometer

Experiment. J. Geophys. Res. 85:8039-8058.

Lacis, A. A. 1975. Cloud structure and heating rates in the atmosphere of Venus. J. Atmos. Sci. 32:1107-1124.

Marov, M. Ya. 1972. Venus: A perspective at the beginning of planetary exploration. Icarus 16:415-461.

Marov, M. Ya., Avduevsky, V. S., Borodin, N. F., Ekonomov, A. P., Kerzhanovich, V. V., Lysov, V. P., Moshkin, B. Ye., Rozhdestvensky, M. K., and Ryabov, O. L. 1973. Preliminary results on the Venus atmosphere from the Venera 8 descent module. Icarus 20:407-421.

Marov, M. Ya., Lebedov, V. N., Lysentsev, V. E., Kuznetsov, I. S., and Popanopulo, G. K. 1976.

Mayer, C. H., McCullough, T. P., and Sloanaker, R. M. 1958. Observations of Venus at 3.15 cm wavelength. Astrophys. J. 127:1-10.

Moroz, V. I., Golovin, Yu. M., Ekonomov, A. P., Moshkin, B.E., Parfent'ev, N. A., and Sanko, N. F. 1980. Spectrum of the Venus day sky. Nature, 284:243.

Moroz, V. I., Parfent'ev, N. A., and San'ko, N. F. 1979. Spectrophotometric experiment in the Venera 11 and Venera 12 descent modules:2. Analysis of Venera 11 spectra by layer-addition method. Kosmicheskie Issledovaniza, 17:727-742.

Moshkin, B. E., Ekonomov, A. P., and Golovin, Yu, M. 1978. Spectral Compositin of Solar Radiation in Venus' Atmosphere According to Light Intensity Measurements on Venera 9 and Venera 10. Cosmic Res. 16:412-418.

Opik, E. J. 1961. The abolosphere and atmosphere of Venus. J. Geophys. Res. 66:2807-2819.

Oyama, V. I., Carle, G. C., Woeller, F., Pollack, J. B., Reynolds, R. T., and Craig, R. A. 1980. Pineer Venus gas chromatography of the lower atmosphere of Venus. J. Geophys. Res. 85:7891-7902.

Pollack, J. B. 1969. A non-gray CO_2-H_2O greenhouse model of Venus. Icarus 10:314-341.

Pollack, J. B., Erickson, E. F., Goorvitch, D., Baldwin, B. J., Stecker, D. W., Witteborn, F.C., and Augason, G. C. 1975. A determination of the composition of the Venus clouds from aircraft observations in the near infrared. J. Atmos. Sci. 32:1140-1150.

Pollack, J. B., Toon, O. B., and Boese, R. 1980. Greenhouse models of Venus' high surfacae temperature, as constrained by Pioneer Venus measurements. J. Geophys. Res. 85:8223-8231.

Pollack, J. B. and Young, R. 1975. Calculations of the radiative and dynamical state of the Venus atmosphere. J. Atmos. Sci. 32:1025-1037.

Revercomb, H. E., Sromovsky, L. A. and Suomi, V. E. 1982. Reassessment of Net Radiation Measurements in the Atmosphere of Venus. Icarus (in press).

Rossow, W. B., Del Genio, A. D., Limaze, S. J., Travis, L. D., and Stone, P. H. 1980. Cloud morphology and motions from Pioneer Venus images. J. Geophys. Res. 85:8107-8128.

Sagan, C. 1960. The surface temperature of Venus. Astron. J. 65:353-353.

Samuelson, R. E. 1967. Greenhouse effect in semi-infinite scattering atmospheres: Application to Venus. Astrophys. J. 147:782-798.

Schofield, J. T. and Taylor, F. W. 1982. Net global thermal emission from the Venusian upper atmosphere. Icarus (in press).

Schubert, G., Covey, C., Del Genio, A., Elson, L. S., Keating, G., Seiff, A., Young, R. E., Apt, J., Counselman III, C. C., Kliore, A. J., Limaye, S. S., Revercomb, H. E., Sromovsky, L. A., Suomi, V. E., Taylor, F., Woo, R., and von Zahz, U. 1980. Structure and circulation of the Venus atmosphere. J. Geophys. Res. 85:8007-8025.

Seiff, A., Kirk, D. B., Young, R. E., Blanchard, R. C., Findlay, J. T., Kelly, G. M., and Sommer, S. C. 1980. Measurements of thermal structure and

thermal contrasts in the atmosphere of Venus and related dynamical observations: Results from the four Pioneer Venus probes. J. Geophys. Res. 85:7903-7933.

Sill, G. 1972. Sulfuric acid in the Venus clouds. Comm. Lunar Planet. Lab. 9:191-198.

Stone, P. H. 1975. The Dynamics of the Atmosphere of Venus. J. Atmos. Sci. 32:1005-1016.

Suomi, V. E., Sromovsky, L. A., and Revercomb, H. E. 1980. Net radiation in the atmosphere of Venus: Measurements and interpretation;. J. Geophys. Res. 85:8200-8218.

Taylor, F. W., Beer, R. Chahine, M.T., Diner, D. J., Elson, L. J., Haskins, R. D., McCleese, D. J., Martonchik, J., Reichley, P. E., Bradley, S. P., Delderfield, J., Schofield, J. T., Farmer, C. B., Froidevaux, L., Leung, J., Coffey, M. T., and Gille, J. E. 1980. Structure and meteorology of the middle atmosphere of Venus: Infrared remote sensing from the Pioneer Orbiter. J. Geophys. Res. 85:7963-8006.

Toksoz, M. N., Hsui, A. T., and Johnson, D. H. 1978. Thermal evolutions of the terrestrial planets. Moon and Planets, 18:281-320.

Tomasko, M. G., Boese, R., Ingersoll, A. P., Laacis, A. A., Limaye, S. S., Pollack, J. B., Seiff, A., Stewarat, A. I., Suomi, V. E., and Taylor, F. W. 1977. The thermal balance of the atmosphere of Venus. Space Sci. Revs. 20:389-412.

Tomasko, M. G., Doose, L. R., and Smith, P. H. 1979. Absorption of sunlight in the atmosphere of Venus. Science 205:80-82.

Tomasko, M., Smith, P., Rayent, B., Esposito, L., McCleese, D., Martonchik, J., and Beer, R. 1980. The clouds of Venus: A synthesis report. J. Geophys. Res. 85:8059-8081.

Tomasko, M. G., Doose, L. R., Smith, P. H., and Odell, A. P. 1980.

Measurements of the flux of sunlight in the atmosphere of Venus. J. Geophys. Res. 85:8167-8186.

Tomasko, M. G., Smith, P. H., Suomi, V. E., Sromovsky, L. A., Revencomb, H. E., Taylor, F. W., Martonchik, J. V., Seiff, A., Boese, R., Pollack, J. B., Ingersoll, A. P., Schubert, G., and Covey, C. C. 1980. The thermal balance of Venus in light of the Pioneer Venus mission. J. Geophys. Res. 85:8187-8199.

Toon, O. B. and Blamont, J. 1982. Large solid particles in the clouds of Venus: Do they exist? Icarus (in press).

Toon, O. B., Ragent, B., Colburn, D., Blamont, J. and Cot, C. 1982. Large, Solid Particles in the Clouds of Venus: Do They Exist? Icarus (in press).

Toon, O. B., and Turco, R. P. 1982. The Ultraviolet Absorber on Venus: Amorphous Sulphur. Icarus (in press).

Young, A. T. 1975. The clouds of Venus. J. Atmos. Sci. 32:1125-1132.

Young, A. T. 1980. Possible explanation of large thermal fluxes measured from Pioneer Venus entry probes. Bull. Amer. Astron. Soc. 12:717.

Young, L.D.G. and Young, A. T. 1973. Comment on the composition of the Venus cloud tops in light of recent spectroscopic data. Astrophys. J. 179:L39-L43.

Young, L.D.G. and Young, A. T., Sanko, N. F. and Zasova, L. V. 1982. A new interpretation of the Venera 11 spectra of Venus. Icarus (in press).

Figure Captions

Fig. 1. Comparison of temperature profiles from the four Pioneer Venus probes. SZA is the solar zenith angle. (From Seiff et al. 1980.)

Fig. 2. Profiles of static stability of the lower atmosphere of Venus from measurements by the Pioneer Venus probes. Positive values indicate stability. The solid lines are from cubic spline fits to the temperature data. Points indicate slopes taken graphically from T(Z) plots. (From Seiff et al. 1980.)

Fig. 3. Net solar flux at the surface of Venus as a function of the cosine of the solar zenith angle. Dashed lines represent constant fractions of the incident solar flux as indicated. The solid line represents the variation computed for a forward scattering cloud model adjusted to pass through the Pioneer Venus measurement at the Large probe site (labeled PV). This measurement and those measured at the Venera 8 (labeled V8), Venera 9 and 10 (V9,10), and Venera 11 and 12 (V11,12) sites are quite consistent. (From Tomasko et al. 1980b.)

Fig. 4. The thermal net flux measurements as published by Suomi et al. 1980) at the three Pioneer Venus small probe entry sites (labeled Night, North, and Day) compared with estimates of the globally averaged bolometric net solar flux based on measurements at the Pioneer Venus Large probe entry site. The solar flux measurements scaled up to include energy outside the passband of the instrument and averaged over the planet using a forward scattering cloud model are labeled "nominal solar". Also shown is

the highest solar net flux profile (labeled high solar) consistent with instrument calibration uncertainties. The long dashed curve above 60 km altitude is a model solar flux calculation. The triangle and dot correspond to estimates of the net thermal and solar flux (respectively) at the top of the atmosphere by the PV orbiter. The magnitudes of the net fluxes are plotted; the solar net flux is directed downward, and the thermal net fluxes are directed upward. (From Tomasko et al. 1980b.)

Fig. 5. Thermal net flux measurements from the three small Pioneer Venus probes after correction for instrumental effects (from Revercomb et al. 1982). The fluxes are compared to radiative transfer calculations for the indicated values of the water mixing ratio. Also shown is the "high" global average solar net flux profile from Fig. 4. The uncertainty of the corrected thermal fluxes depends on the uncertainty in the model computed fluxes at 14 km. This effect gives an estimated uncertainty of 10 W m^{-2} at 14 km with decreasing uncertainty at increasing altitude.

Fig. 6. The ratio of infrared absorption cross section to extinction cross section in the visible (0.63 um) as a function of wavelength for sulfuric acid droplets having the size distributions measured for mode 2 (effective particle diameter, d = 2.1 um) mode 2' (d = 2.8 um) and mode 3 (d = 6.7 um). Also shown are the blackbody emission curves (dashed lines) for 270 K and 380 K, the temperatures at the base of the upper and lower cloud layers, respectively. (From Tomasko et al. 1980b.)

Fig. 7. a) A comparison of zonal wind velocity profiles from Pioneer Venus and Venera probes. (From Schubert et al. 1980.) (b) meridional wind profiles from Pioneer Venus (DLBI) and Doppler tracking data. (From

Counselman et al. 1980.)

Fig. 8. Comparison of the observed temperature structure in Venus's lower atmosphere with that of several one-dimensional radiative-convective models. The "base case" uses the Venera 11 water vapor profile and the PV "high solar" net flux profile. The "altered solar flux" model uses the somewhat lower "nominal solar" net flux profile from PV. The "enhanced water vapor" model uses the water vapor measured by Oyama et al. (1980b). (From Pollack et al. 1980a.)

Fig. 9. Comparison between the observed stability structure of Venus's lower atmosphere and that of the models shown in Fig. 8. The stability parameter equals the difference between the adiabatic and actual lapse rates. At all altitudes from 0 to 80 km, where a given theoretical curve is not explicitly illustrated, the stability parameter equals zero. (From Pollack et al. 1980a.)

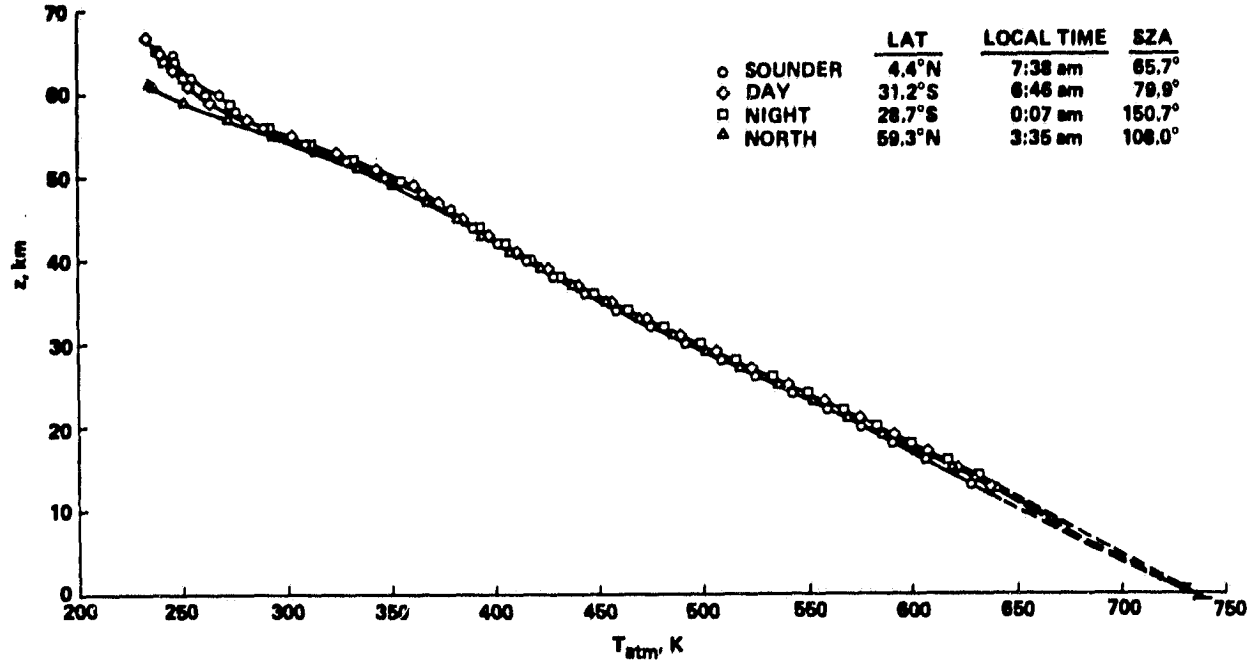

Fig. 1

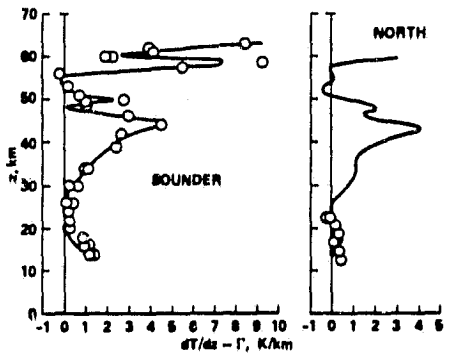

Fig. 17a

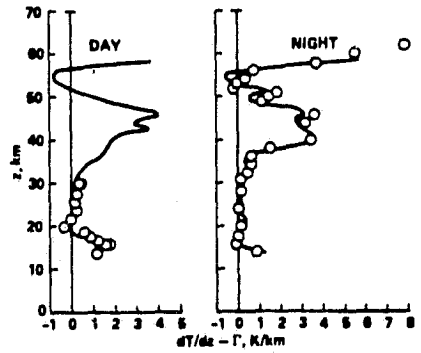

Fig. 2

ORIGINAL PAGE IS
OF POOR QUALITY

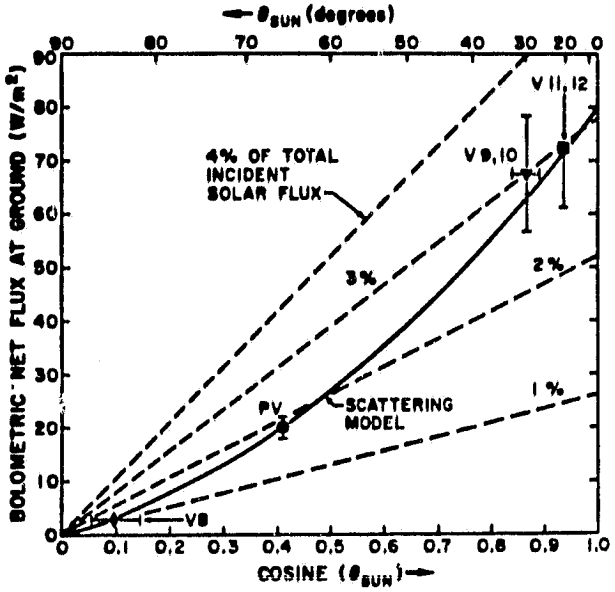

Fig. 3

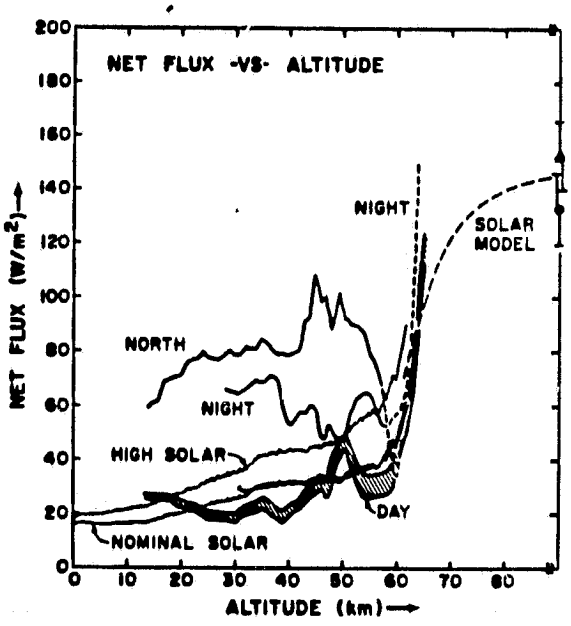

Fig. 4

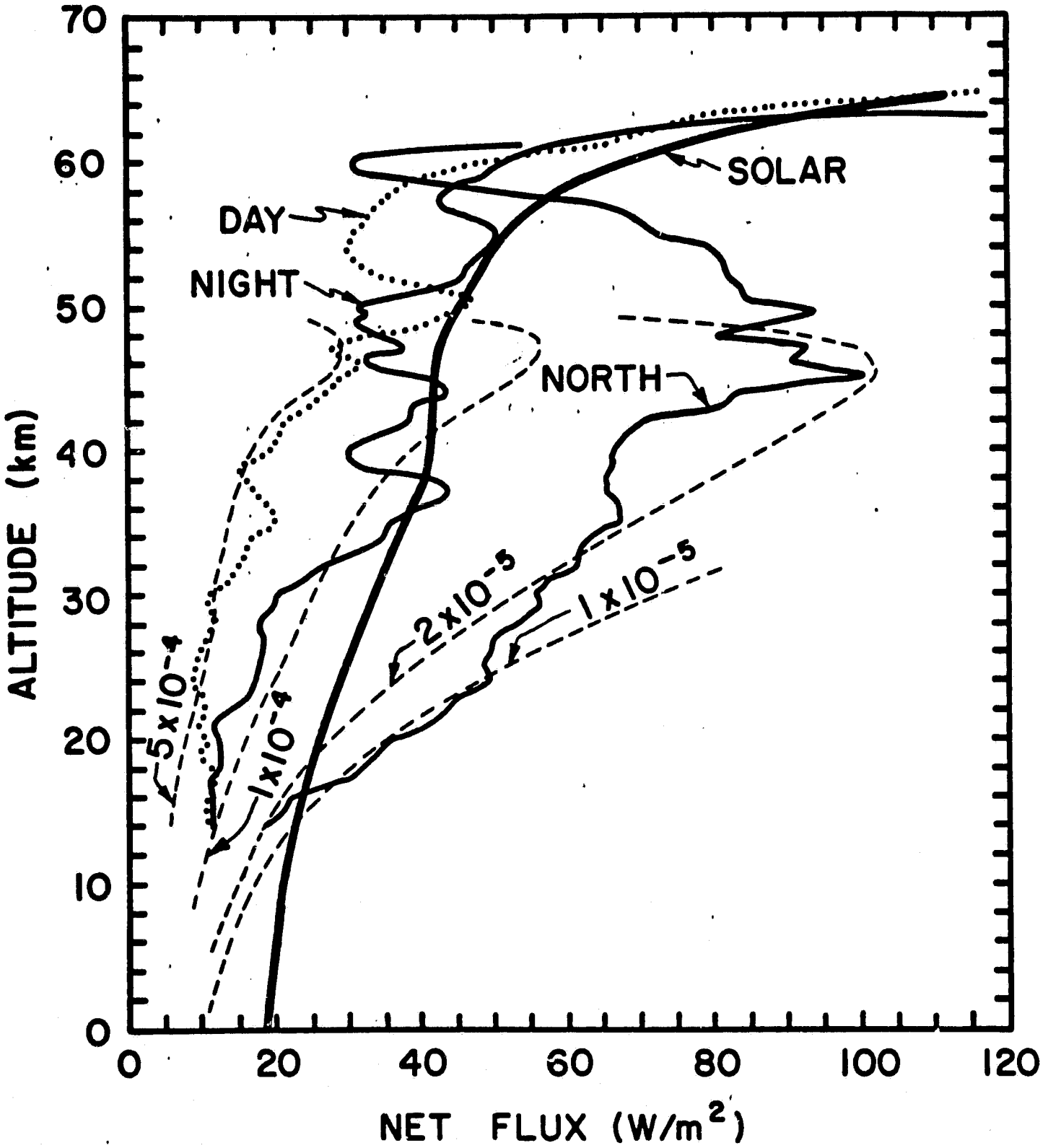

Figure 10.

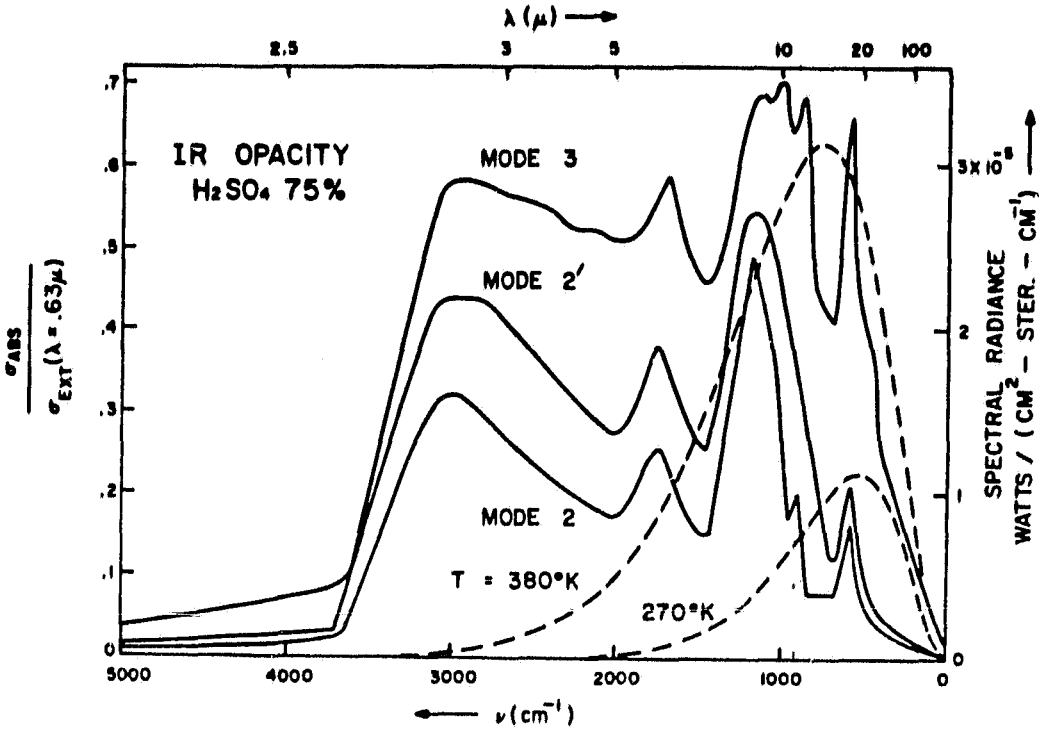

Fig. 5 6

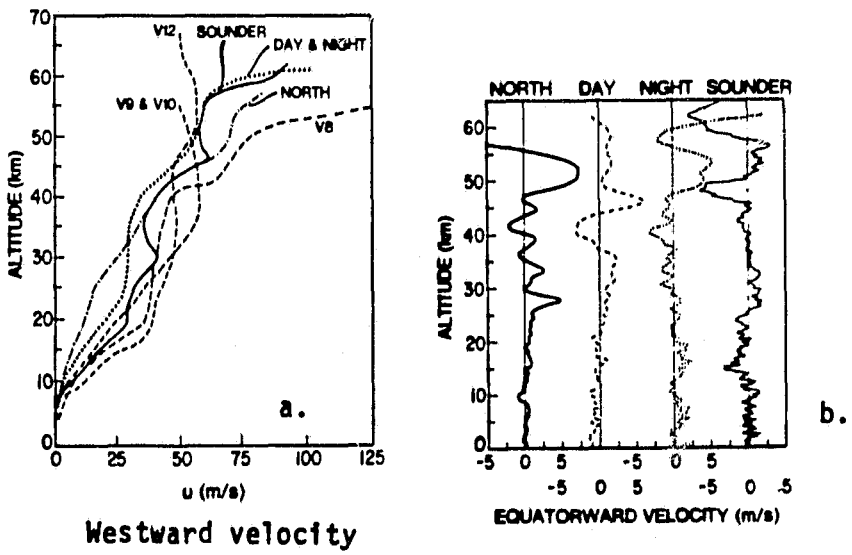

Fig. 6 7

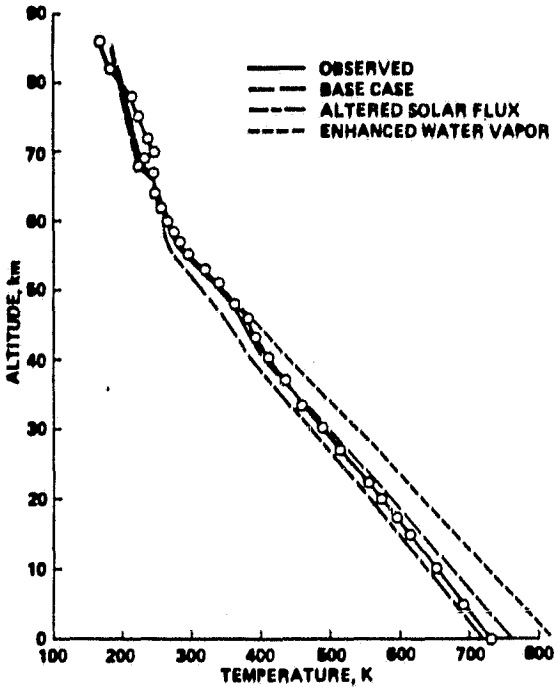

Fig. 7 8

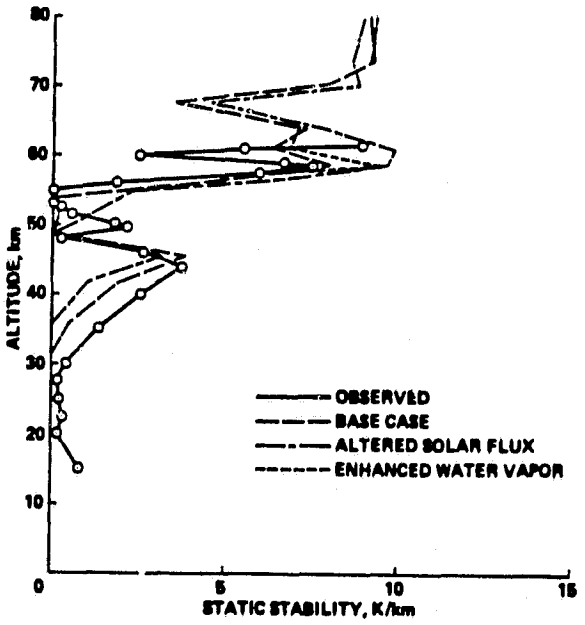

Fig. 8 9